Langmuir

ARTICLE

pubs.acs.org/Langmuir

Surface-Enhanced Raman Scattering of 4-Aminobenzenethiol in Ag Sol: Relative Intensity of a_1- and b_2-Type Bands Invariant against Aggregation of Ag Nanoparticles

Kwan Kim,*[,†] Jae Keun Yoon,[†] Hyang Bong Lee,[†] Dongha Shin,[†] and Kuan Soo Shin*[,‡]

[†]Department of Chemistry, Seoul National University, Seoul 151-742, Korea

[‡]Department of Chemistry, Soongsil University, Seoul 156-743, Korea

ABSTRACT: 4-Aminobenzenthiol (4-ABT) is an unusual molecule, showing variable surface-enhanced Raman scattering (SERS) spectra depending upon measurement conditions. In an effort to reduce ambiguity and add clarity, we have thus conducted an ultraviolet−visible (UV−vis) extinction measurement, along with Raman scattering measurement, after adding 4-ABT into aqueous Ag sol. Upon the addition of 4-ABT, the surface plasmon absorption band of Ag at 410 nm gradually diminished and, concomitantly, a weak and broad band developed at longer wavelengths, obviously because of the aggregation of Ag nanoparticles. At the same time, the Raman scattering peaks of 4-ABT varied in intensity as the Ag particles proceeded to form aggregates. A close examination revealed that the peak intensity of the ring 7a band of 4-ABT, a typical a_1 vibrational mode, could be correlated with the UV−vis extinction of the Ag sol measured at the excitation laser wavelength. In a separate Raman measurement conducted using sedimented Ag colloidal particles, 4-ABT was found not to be subjected to any surface-induced photoreaction, implying that all of the observable Raman peaks were, in fact, solely due to 4-ABT on Ag. The intensities of the b_2-type bands, such as the ring 3, 9b, and 19b modes of 4-ABT, were then analyzed and found to be invariant with respect to the 7a band, irrespective of the extent of Ag aggregation as far as at a fixed excitation wavelength. The intensity ratio of the b_2-type/7a bands would then reflect the extent of the chemical enhancement that was involved in the SERS of 4-ABT in aggregated Ag sol.

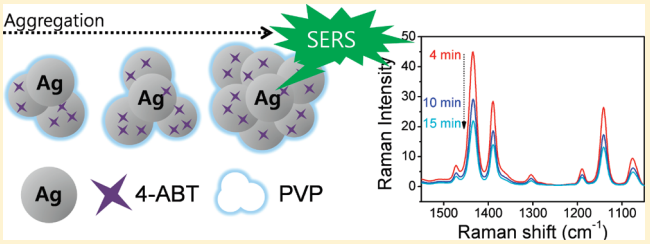

INTRODUCTION

Noble metallic nanostructures exhibit a phenomenon known as surface-enhanced Raman scattering (SERS), in which the scattering cross-sections are dramatically enhanced for molecules adsorbed thereon.[1−3] In recent years, it has been reported that even single-molecule spectroscopy is possible by SERS, suggesting that the enhancement factor (EF) can reach as much as 10^{14}−10^{15}.[4−7] According to theoretical studies, at least 8−10 orders of magnitude can arise from electromagnetic surface plasmon excitation,[7,8] in addition to any chemical enhancement associated with either the metal−molecule or molecule−metal charge-transfer transition. Lombardi and Birke[9,10] have shown recently that SERS intensity can be expressed as a function of the product of three contributions, representing the surface plasmon resonance, the metal−molecule charge-transfer resonance at the Fermi energy, and an allowed molecular resonance. There is then a possibility that the charge-transfer contribution may dominate the SERS spectrum.

4-Aminobenzenethiol (4-ABT) is an unusual molecule in the sense that its SERS spectral feature is dependent upon not only the kinds of SERS substrates but also the measurement conditions.[11−15] Specifically, ever since Osawa et al.[11] reported the potential and wavelength-dependent SERS spectra of 4-ABT on a silver electrode 2 decade ago, it has been regarded as a model adsorbate for probing the chemical enhancement mechanism in SERS. This is because, in the normal Raman spectrum of 4-ABT, only peaks assignable to totally symmetric (a_1) vibrations are observed, but in its SERS spectrum, several additional lines are identified that can be attributed to b_2 symmetry. Osawa et al.[11] reasoned that the appearance of strong lines of b_2 symmetry is due to intensity, borrowing from an intense $\pi \rightarrow \pi^*$ molecular transition ($^1A_1 \rightarrow {}^1B_2$) at 300 nm. In line with this reasoning, Lombardi and Birke[9,10] explained the observed spectrum of 4-ABT using only the Herzberg−Teller surface selection rules. They even figured out the relative charge-transfer contribution to SERS in 4-ABT. Very recently, however, many researchers have arrived at a different explanation for the appearance of b_2-type bands.[12−15]

On the basis of an *ab initio* molecular orbital calculation, Wu et al.[16] reported that *p*,*p*′-dimercaptoazobenzene (DMAB) could be produced from 4-ABT by a catalytic coupling reaction on silver nanoparticles. A similar conclusion was reached by Fang et al.[17] by comparing the calculated Raman spectrum of DMAB with the experimental spectrum of 4-ABT in Ag sol. To support

Received: January 22, 2011
Revised: February 27, 2011
Published: March 15, 2011

these theoretical predictions, Huang et al.[18] synthesized DMAB and compared its SERS spectrum to that of 4-ABT. They claimed that the SERS spectral pattern of DMAB is almost the same as that of 4-ABT. Furthermore, they reported that the surface mass spectrum of 4-ABT on Ag, measured after illumination with a high-power laser, showed a peak corresponding to DMAB,[18] thus concluding that the b_2-type bands claimed by Osawa et al. are not due to 4-ABT after all but due to the A_g modes of DMAB produced from 4-ABT. Although DMAB might be formed from 4-ABT on Ag by the irradiation of a visible laser, there was no proposed mechanism that could explain the reaction properly.

Recently, we and others have investigated the SERS of 4-ABT positioned in the gap of metal nanostructures.[19−21] When 4-ABT is adsorbed on a flame-annealed Au substrate, no Raman peak is identifiable, but because silver or gold nanoparticles are adsorbed further onto the pendent amine groups of 4-ABT, a very intense Raman spectrum is obtained. In our research, not only the a_1-type bands but also the b_2-type bands of 4-ABT were distinctly observed in these spectra.[19−21] Considering the fact that an azo compound in *cis* configuration would be energetically unfavorable on an atomically flat gold terrace,[22,23] it is unlikely that the b_2-type bands observed are due to the formation of DMAB. Because the SERS spectral pattern of 4-ABT even in Ag sol is comparable to that in a nanogap system, it is questionable whether the b_2-type bands are due to DMAB.

We have accordingly re-examined the SERS spectra of 4-ABT in Ag sol. First, by conducting a coupled ultraviolet−visible (UV−vis) extinction and Raman spectral measurement, we reveal that the intensity ratio of the b_2-/a_1-type bands is independent of the extent of the aggregation of Ag nanoparticles, at least at a fixed excitation wavelength. Second, by conducting a Raman spectral measurement under spinning of sedimented colloidal Ag particles, we reveal that the appearance of the so-called b_2-type bands has nothing to do with the surface-induced photoreaction. Their appearance must then be intrinsic to 4-ABT (not because of photo-produced DMAB), associated with the chemical enhancement mechanism in SERS. The b_2/a_1 band intensity ratio and not their absolute intensity can therefore be used as a measure to quantify the extent of chemical enhancement in the SERS of 4-ABT.

EXPERIMENTAL SECTION

Silver nitrate ($AgNO_3$, 99%), trisodium citrate (99%), 4-ABT (97%), 4-nitrobenzenethiol (4-NBT, 80%), poly(vinylpyrollidone) (PVP, MW of ∼55 000), and poly(allylamine hydrochloride) (PAH, MW of ∼70 000) were purchased from Aldrich and used as received. The chemicals, unless specified, were all reagent-grade, and triply distilled water of resistivity greater than 18.0 MΩ cm was used throughout.

An Ag sol was prepared by following the modified recipe by Lee and Meisel.[24] At first, 150 mL of 0.67 mM $AgNO_3$ solution was heated to boil. A solution of 0.12 mM sodium citrate (0.833 mL) was added therein under vigorous stirring, and the boiling was continued for 40 min. The sampling solution of Raman spectral measurements was prepared by mixing 20 μL of ethanolic 4-ABT solution with 980 μL of Ag sol and then allowing the Ag nanoparticles therein to aggregate for a certain period of time before adding 1 μL of 1% (w/v) PVP solution as a colloid stabilizer to prevent their further aggregation.

UV−vis extinction spectra were obtained using a SCINCO S-4100 spectrometer. Atomic force microscope (AFM) images were obtained on a Digital Instruments Nanoscope IIIa system. Using a 125 μm long etched silicon cantilever with a nominal spring constant of 20−100 N/m (Nanoprobe, Digital Instruments), topographic images were recorded in a tapping mode with a driving frequency of ∼300 kHz at a scan rate of 1 Hz. Infrared spectra were obtained using a Bruker IFS 113v FTIR spectrometer equipped with a Globar light source and a liquid-N_2-cooled wide-band mercury cadmium telluride detector. Raman spectra were obtained using a Renishaw Raman system model 2000 spectrometer equipped with an integral microscope (Olympus BH2-UMA). The 514.5 nm line from a 20 mW Ar^+ laser (Melles-Griot model 351MA520), the 568 nm line from a 20 mW Ar^+/Kr^+ laser (Melles-Griot model 35KAP431), or the 632.8 nm line from a 17 mW He/Ne laser (Spectra Physics model 127) was used as the excitation source, and the Raman scattering was detected over a 180° range with a Peltier cooled (−70 °C) charged-coupled device (CCD) camera (400 × 600 pixels). The holographic grating (1800 grooves/mm) and the slit allowed the spectral resolution to be 1 cm^{-1}. The Raman band of a silicon wafer at 520 cm^{-1} was used to calibrate the spectrometer.

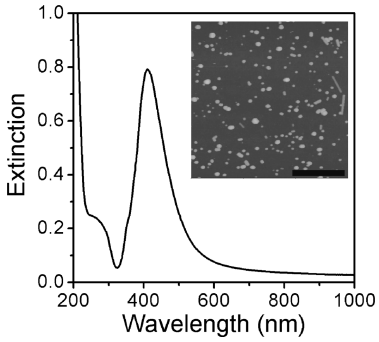

Figure 1. UV−vis extinction spectrum of Ag nanoparticle solution. The inset is an AFM image of Ag nanoparticles (scale bar = 1 μm).

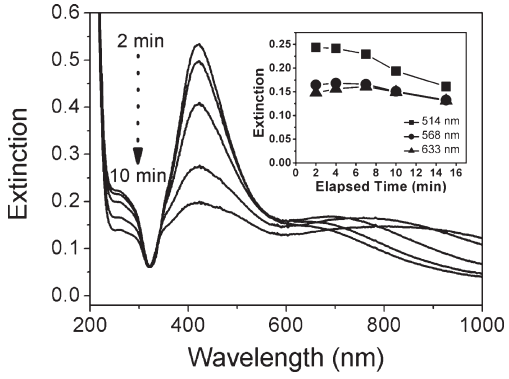

Figure 2. UV−vis extinction spectra of Ag sol measured 2, 4, 7, 10, or 15 min later after the addition of 4-ABT into the sol, finally stabilizing by PVP. The inset shows the absorbances at 514.5, 568, and 632.8 nm drawn versus the duration of time elapsed before adding PVP.

RESULTS AND DISCUSSION

The inset of Figure 1 shows the AFM image of Ag nanoparticles prepared in this work. The particles are mostly spherical, with an average diameter of ∼35 nm. These spherical particles exhibit their surface plasmon band at 411 nm, as seen in Figure 1. Considering the initial amount of silver nitrate used to prepare the Ag sol, the concentration of Ag nanoparticles is estimated to be 0.48 nM. Assuming then that 4-ABT adsorbs on Ag very favorably, occupying an area of 0.20 nm^2/molecule,[25] we added 4-ABT into the Ag sol, so that it covered ∼70% of the colloidal surfaces. Subsequently, the 4-ABT-adsorbed Ag sol was allowed

dx.doi.org/10.1021/la200293b |*Langmuir* 2011, 27, 4526–4531

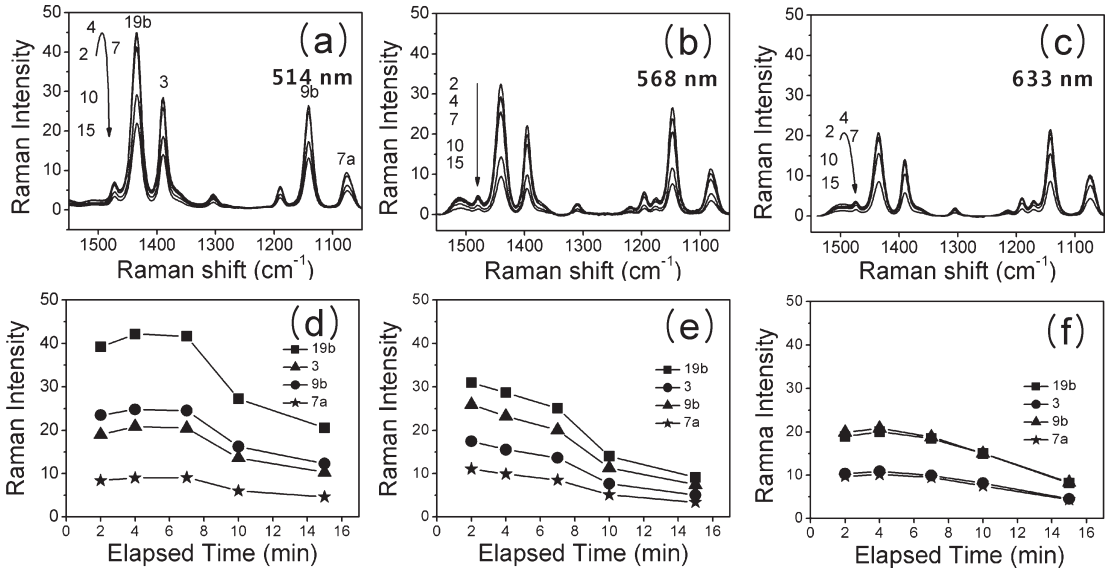

Figure 3. Raman spectra of 4-ABT measured 2, 4, 7, 10, or 15 min later after its addition to Ag sol using (a) 514.5 nm, (b) 568 nm, and (c) 632.8 nm laser as the excitation source. Panels d, e, and f represent the peak intensity changes measured for the 19b, 3, 9b, and 7a bands in panels a, b, and c, respectively.

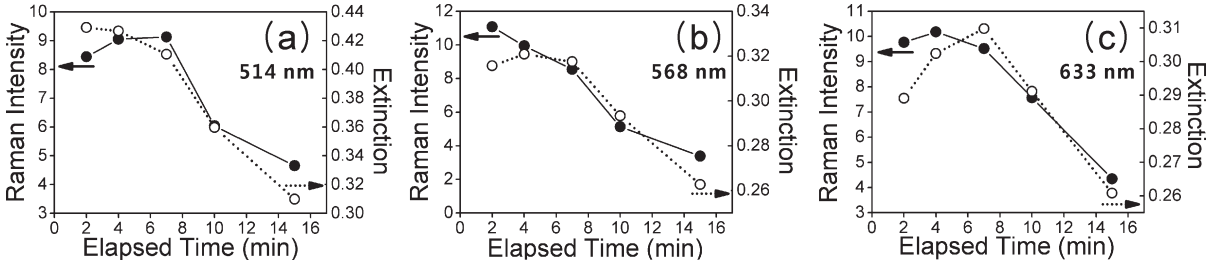

Figure 4. Variation of Raman peak intensity of the 7a band (●) measured at (a) 514.5 nm, (b) 568 nm, and (c) 632.8 nm excitation, drawn along with the associated UV−vis extinction spectral profile (○).

to aggregate for 2, 4, 7, 10, or 15 min, after which PVP was added to prevent further aggregation of the Ag particles; hereafter, the resulting solutions were labeled as Ag sol (2 min), Ag sol (4 min), Ag sol (7 min), Ag sol (10 min), and Ag sol (15 min), respectively.

Figure 2 shows UV−vis extinction spectra of the 4-ABT-adsorbed Ag colloids stabilized by PVP. The UV−vis spectral feature varies as a function of time elapsed before adding PVP. As more time is allowed, the band located at ∼410 nm weakens progressively and a broad band develops in the region of longer wavelengths instead. These changes are due to the aggregation of Ag nanoparticles originating from the ligand exchange of citrate ions with 4-ABT. The inset in Figure 2 shows the variation of the UV−vis absorbances at 514.5, 568, and 632.8 nm, corresponding to three different Raman excitation wavelengths used in this work, as a function of time allowed for the aggregation of Ag nanoparticles. The absorbance at 514.5 nm represented the greatest and most rapid change, followed in order by those at 568 and 632.8 nm.

The Raman spectra of Ag sol (2 min), Ag sol (4 min), Ag sol (7 min), Ag sol (10 min), and Ag sol (15 min) acquired using 514.5, 568, and 632.8 nm excitation are shown in panels a, b, and c of Figure 3, respectively. All of the spectra are dominated by four bands. If no reaction has occurred, three of them at 1140, 1390, and 1430 cm^{-1} can be attributed to the b_2-type ring 9b, 3, and 19b modes of 4-ABT, respectively, while the remaining one at 1080 cm^{-1} is due to the a_1-type ring 7a mode.[11] Overall, a more intense spectrum was measured by excitation with radiation of 514.5 > 568 > 632.8 nm in that order. However, at a fixed excitation wavelength, the Raman signal was subject to change depending upon the length of time allowed for Ag nanoparticles to aggregate, obviously decreasing for Ag sol (10 min) and Ag sol (15 min). This is seen more clearly in panels d−f of Figure 3, which show the variation of the peak intensities in panels a−c of Figure 3, respectively. We can notice that the peak intensity variation (in panels d−f of Figure 3) and the excitation wavelength dependence of Raman signal (in panels a−c of Figure 3) correlate fairly well with the UV−vis extinction spectral changes (summarized in the inset of Figure 2).

It has generally been accepted that electromagnetic enhancement in SERS is deeply associated with the surface plasmon resonance of metal particles and their aggregates and, thus, that the electromagnetic effect must correlate with the extinction spectral profile.[26] According to Osawa et al.,[11] the a_1-type bands of 4-ABT, such as the ring 7a band, should exclusively exhibit this electromagnetic enhancement when the molecule is adsorbed on Ag, while the b_2-type bands, such as 3, 9b, and 19b bands, are further affected by chemical enhancement. To confirm the feasibility of this idea, we have compared the variation of the 7a band intensity (in panels d−f of Figure 3) to the extinction

dx.doi.org/10.1021/la200293b |Langmuir 2011, 27, 4526–4531

spectral profiles (in the inset of Figure 2). In fact, as shown in panels a−c of Figure 4, the full lines exhibiting the variation of the 7a band intensity correlate fairly well to the dotted lines that exhibit the changes in extinction behavior. A small disagreement seen in the earlier aggregation time may be due to the disturbance of 4-ABT on Ag.

As mentioned in the Introduction,[16−18] there is a debate recently as to whether the b_2-type bands are intrinsically due to 4-ABT or are derived from a photoreaction product, such as DMAB. To resolve the argument, we have conducted two control experiments, one using 4-NBT and the other using 4-ABT. It is well-known that 4-NBT in Ag sol is subjected to photoreaction, exhibiting a SERS spectrum very similar to that of 4-ABT. This is evident from curves a and b of Figure 5, which show, respectively, the normal Raman spectrum and the SERS spectrum of 4-NBT in Ag sol taken using 514.5 nm radiation as the excitation source. The NO_2 stretching band because of 4-NBT adsorbed on Ag is observable at 1330 cm^{-1} in the SERS spectrum,[27] but additional bands due to a photoreaction product are also observed. Notice that the bands marked with asterisks (*) in curve b of Figure 5 resemble the b_2-type bands of 4-ABT in Figure 3, suggesting that 4-NBT on Ag is converted to 4-ABT. To minimize the surface-induced photoreaction, we carried out subsequent experiments under spinning.

For that purpose, a fresh 4-NBT-adsorbed Ag sol was newly centrifuged and the precipitate was mixed with KBr powder and made into a pellet. Curve c of Figure 5 shows the Raman spectrum of the pellet measured under spinning at 3000 rpm; the laser power at the sampling position was 0.2 mW. All of the peaks in curve c of Figure 5 can be attributed to 4-NBT on Ag. No bands because of a photo-product are identifiable in this spectrum. Curve d of Figure 5 shows the Raman spectrum of the pellet taken in a static condition. In this case, peaks because of the photoreaction are clearly seen. In comparison to curve b of Figure 5, the photoreaction is presumed to occur more favorably under ambient conditions than in water. Anyhow, clearly the surface-induced photoreaction can be minimized by spinning the sample. In this light, we also prepared a KBr pellet, including 4-ABT-adsorbed Ag nanoaggregates. Curve e of Figure 5 shows the Raman spectrum of the pellet measured under spinning at 3000 rpm, while curve f of Figure 5 shows the spectrum measured in a static condition. Clearly, the b_2-type bands are observed irrespective of spinning. In practice, there is no difference at all between the two spectra. This suggests that actually no photoreaction took place even during the acquisition of the static spectrum. Although not shown here, the infrared spectrum of the pellet was also not subject to change, even after a prolonged exposure to a Hg lamp. Consulting the photoreaction characteristics of 4-NBT shown in curves b and d of Figure 5, 4-ABT might be more difficult to photoreact in the aqueous phase. We thus presume that the b_2-type bands seen in Figure 3 are all due to 4-ABT and not due to a photoreaction product, such as DMAB. On these grounds, the SERS peak intensities shown in Figure 3 were further analyzed.

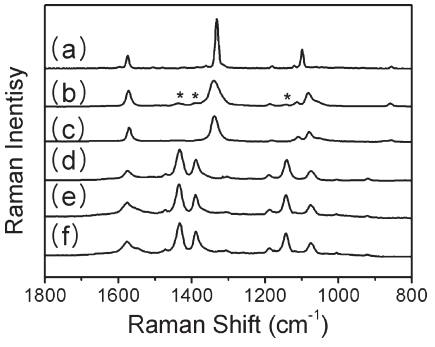

Figure 5. (a) Normal Raman and (b) SERS spectrum of 4-NBT in Ag sol. Raman spectra of a KBr pellet containing 4-NBT-adsorbed Ag nanoparticles (c) taken under spinning at 3000 rpm and (d) taken in static condition. Raman spectra of a KBr pellet containing 4-ABT-adsorbed Ag nanoparticles (e) taken under spinning at 3000 rpm and (f) taken in static condition. All spectra were taken using 514.5 nm radiation as the excitation source.

As seen in panels d−f of Figure 3, the b_2-type bands lose intensity as a function of aggregated time, in a manner similar to the 7a band. Considering that the b_2-type bands are affected by both the electromagnetic and chemical enhancement, contrary to the case of the 7a band, it is much better to examine their intensity variation after normalizing with respect to that of the 7a band. As seen in Figure 6, the normalized peak intensities of the b_2-type bands are fairly invariant with respect to the aggregation of Ag nanoparticles, irrespective of the Raman excitation wavelength. This implies that they are free from electromagnetic enhancement. If any photoreaction took place during the spectral measurement, the normalized peak intensities might have shown a scattered variation. On this basis, we plotted, shown in Figure 7, the normalized peak intensities of the 3, 9b, and 19b bands as a function of the excitation wavelength. The data in Figure 7 are reproduced, independent of the order of the excitation wavelengths used to measure Raman spectra, suggesting that the b_2-type bands are not due to any reaction product but, in fact, due to 4-ABT. Clearly, all of the b_2 modes become less enhanced as the excitation wavelength is increased. Not only an energy-matching condition but also the photoelectron ejection efficiency of Ag nanoparticles might be taken into account to understand the

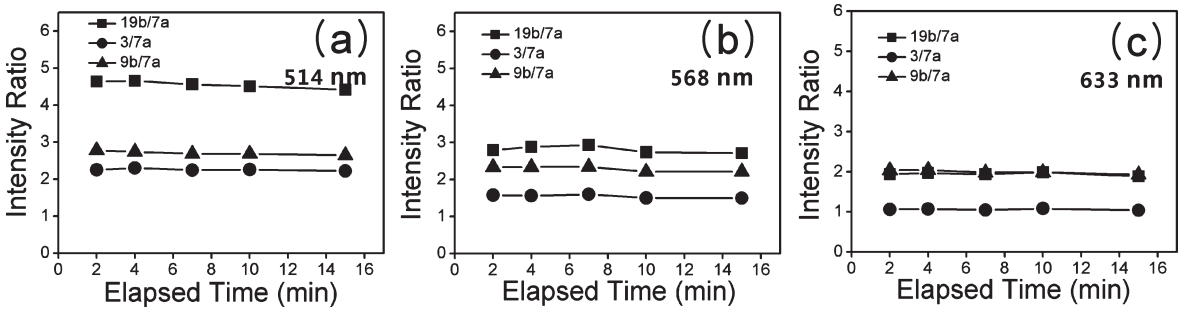

Figure 6. Variation of Raman peak intensities of the b_2-type bands (■, 19b; ●, 3; ▲, 9b) normalized with respect to that of the a_1-type 7a band, measured as a function of aggregation time using (a) 514.5 nm, (b) 568 nm, and (c) 632.8 nm radiation as the excitation source.

dx.doi.org/10.1021/la200293b |*Langmuir* 2011, 27, 4526–4531

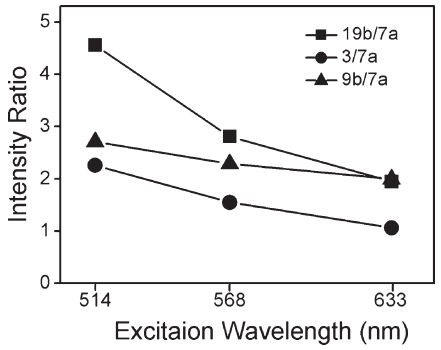

Figure 7. Average values of the normalized peak intensities of the b_2 modes (■, 19b; ●, 3; ▲, 9b) in Figure 6 drawn versus the laser excitation wavelengths.

charge-transfer transition in this case. Anyhow, the pattern of the intensity variation of the ring 19b mode is quite similar to that of the ring 3 mode, although the ring 9b mode shows less dependence upon the excitation wavelength. The latter difference is presumably associated with the fact that the vibrational frequency of the ring 9b mode (~1140 cm^{-1}) deviates significantly from those of the ring 3 (~1390 cm^{-1}) and 19b (~1430 cm^{-1}) modes.

As described above, the b_2-type bands are enhanced via both electromagnetic and chemical enhancement mechanisms, while the a_1-type bands, such as the ring 7a, are enhanced mainly via the electromagnetic enhancement mechanism. Upon this reasoning, the enhancement factors of the 19b and 7a modes, for instance, can be denoted as follows:

$$\begin{aligned} EF_{19b} &= EM_{19b}CHEM_{19b} \\ &= (a_{19b,EM}F_{EM})(a_{19b,CHEM}F_{CHEM}) \end{aligned} \quad (1)$$

$$EF_{7a} = EM_{7a} = a_{7a,EM}F_{EM} \quad (2)$$

in which EF_{mode}, EM_{mode}, and $CHEM_{mode}$ mean the overall, electromagnetic, and chemical enhancement factors (EFs) of the 19b or 7a mode, respectively. Further, the factor $F_{mechanism}$ is presumed to be a collective and universal EF value associated with the referred mechanism in this molecular system. The constant $a_{mode,mechanism}$ is a proper coefficient reserved for the referred mode that is obviously dependent upon the adsorbate orientation. The SERS intensity would then be expressed as follows:

$$I_{SERS,19b} = I_{NR,19b}EF_{19b}(\text{number of 4-ABT molecules}) \quad (3)$$

$$I_{SERS,7a} = I_{NR,7a}EF_{7a}(\text{number of 4-ABT molecules}) \quad (4)$$

in which $I_{NR,\ mode}$ is the normal Raman scattering intensity of the 19b or 7a mode. The ratio of eqs 3 and 4 can then be expressed as follows to represent the intensity ratio of the ring 19b and 7b bands in the SERS of 4-ABT:

$$\begin{aligned} &I_{SERS,19b}/I_{SERS,7a} \\ &= (I_{NR,19b}/I_{NR,7a})(a_{19b,CHEM}a_{19b,EM}/a_{7a,EM})F_{CHEM} \\ &= (I_{NR,19b}/I_{NR,7a})\text{constant}_{19b,7a}\,F_{CHEM} \\ &= \text{constant} \times F_{CHEM} \end{aligned} \quad (5)$$

The fact that the term for the chemical enhancement or F_{CHEM} only remains in eq 5 means that the intensity ratio of the 19b and 7a modes is determined solely by the chemical enhancement; that is, the effect of the electromagnetic enhancement is excluded. Because the adsorbate orientation of 4-ABT on Ag will be negligibly dependent upon the size and shape of the Ag nanoaggregate, the values of the coefficients, $a_{19b,CHEM}$, $a_{19b,EM}$, and $a_{7a,EM}$, are all supposed to be invariant in this system, irrespective of the aggregation of Ag nanoparticles. Hence, it is not unreasonable to observe a rather steady value, as in Figure 6, for the intensity ratio of the b_2-/a_1-type bands. Figure 7 dictates clearly that the F_{CHEM} value should be greater at shorter wavelength excitation.

CONCLUSION

4-ABT is an unusual molecule in the sense that its SERS spectral feature is dependent upon not only the kinds of SERS substrates but also the measurement conditions. The most unambiguous of these factors is the interpretation of the origin of the b_2-type bands. The bands can be interpreted arising from either a surface-induced photoreaction product or purely 4-ABT caused by the involvement of the chemical enhancement mechanism in SERS. To resolve the difficulty, we have carried out a thorough UV−vis and Raman peak analysis for 4-ABT-adsorbed Ag colloidal particles. First of all, in the colloidal state, the Raman peak intensity of 4-ABT was found to vary in conformity with the UV−vis extinction spectra, suggesting the importance of the electromagnetic enhancement mechanism in SERS. Second, when the SERS spectra of 4-ABT-adsorbed sedimented colloidal Ag particles taken under both spinning and static conditions were compared, the appearance of b_2-type bands was clearly rendered by 4-ABT and not because of any photoreaction product, implying the importance of the chemical enhancement mechanism in SERS. On this ground, third, the b_2-type peak intensities normalized with respect to the a_1-type band was found to be invariant with respect to the aggregation of Ag nanoparticles, irrespective of the Raman excitation wavelength. Finally, by modeling an electromagnetically and/or chemically enhanced band, the invariance of the b_2-/a_1-type band intensity ratio was successfully understood. The chemical enhancement thus seemed to be more favorable at shorter wavelength excitations, i.e., 514.5 > 568 > 632.8 nm, at least for 4-ABT adsorbed on colloidal Ag particles. After consultation of the recent SERS study of 4-ABT on Au,[28] the chemical enhancement mechanism must be more dominant at higher laser powers because more 4-ABT molecules can then occupy the chemical enhancement sites.

AUTHOR INFORMATION

Corresponding Author

*Telephone: +82-2-8806651. Fax: +82-2-8891568. E-mail: kwankim@snu.ac.kr (K.K.); Telephone: +82-2-8200436. Fax: +82-2-8244383. E-mail: kshin@ssu.ac.kr (K.S.S.).

ACKNOWLEDGMENT

This work was supported by National Research Foundation of Korea Grants funded by the Korean Government (Grants 2010-0001637, M10703001067-08M0300-06711-Nano2007-02943, KRF-2008-313-C00390, and 2009-0072467).

REFERENCES

(1) Moskovits, M. *Rev. Mod. Phys.* **1985**, *57*, 783.
(2) Kneipp, K.; Wang, Y.; Kneipp, H.; Itzkan, I.; Dasari, R. R.; Feld, M. S. *Phys. Rev. Lett.* **1996**, *76*, 2444.
(3) Kneipp, K.; Kneipp, H.; Itzkan, I.; Dasar, R. R.; Feld, M. S. *Chem. Rev.* **1999**, *99*, 2957.
(4) Nie, S.; Emory, S. R. *Science* **1997**, *275*, 1102.

(5) Xu, H.; Bjerneld, E. J.; Käll, M.; Börjesson, L. *Phys. Rev. Lett.* **1999**, *83*, 4357.
(6) Le Ru, E. C.; Blackie, E.; Meyer, M.; Etchegoin, P. G. *J. Phys. Chem. C* **2007**, *111*, 13794.
(7) Futamata, M.; Maruyama, Y.; Ishikawa, M. *Vib. Spectrosc.* **2002**, *30*, 17.
(8) Jiang, J.; Bosnick, K.; Maillard, M.; Brus, L. *J. Phys. Chem. B* **2003**, *107*, 9964.
(9) Lombardi, J. R.; Birke, R. L. *Acc. Chem. Res.* **2009**, *42*, 734.
(10) Lombardi, J. R.; Birke, R. L. *J. Phys. Chem. C* **2008**, *112*, 5605.
(11) Osawa, M.; Matsuda, N.; Yoshii, K.; Uchida, I. *J. Phys. Chem.* **1994**, *98*, 12702.
(12) Hu, X.; Wang, T.; Wang, L.; Dong, S. *J. Phys. Chem. C* **2007**, *111*, 6962.
(13) Wang, Y.; Chen, H.; Dong, S.; Wang, E. *J. Chem. Phys.* **2006**, *124*, No. 074709.
(14) Zhou, Q.; Li, X.; Fan, Q.; Zhang, X.; Zheng, J. *Angew. Chem., Int. Ed.* **2006**, *45*, 3970.
(15) Huang, Y.; Fang, Y.; Yang, Z.; Sun, M. *J. Phys. Chem. C* **2010**, *114*, 18263.
(16) Wu, D. Y.; Liu, X. M.; Huang, Y. F.; Ren, B.; Xu, X.; Tian, Z. Q. *J. Phys. Chem. C* **2009**, *113*, 18212.
(17) Fang, Y.; Li, Y.; Xu, H.; Sun, M. *Langmuir* **2010**, *26*, 7737.
(18) Huang, Y. F.; Zhu, H. P.; Liu, G. K.; Wu, D. Y.; Ren, B.; Tian, Z. Q. *J. Am. Chem. Soc.* **2010**, *132*, 9244.
(19) Kim, K.; Lee, H. B.; Yoon, J. K.; Shin, D.; Shin, K. S. *J. Phys. Chem. C* **2010**, *114*, 13589.
(20) Yoon, J. K.; Kim, K.; Shin, K. S. *J. Phys. Chem. C* **2009**, *113*, 1769.
(21) Yoon, J. K.; Kim, K. *J. Phys. Chem. B* **2005**, *109*, 20731.
(22) Zhang, C.; Du, M. H.; Cheng, H. P.; Zhang, X. G.; Roitberg, A. E.; Krause, J. L. *Phys. Rev. Lett.* **2004**, *92*, 158301.
(23) Schulze, F. W.; Petrick, H. J.; Cammenga, H. K.; Klinge, H. *Z. Phys. Chem. Neue Folge* **1977**, *107*, 1.
(24) Lee, P. C.; Meisel, D. *J. Phys. Chem.* **1982**, *86*, 3391.
(25) Gole, A.; Sainkar, S. R.; Sastry, M. *Chem. Mater.* **2000**, *12*, 1234.
(26) Anker, J. N.; Hall, W. P.; Lyandres, O.; Shah, N. C.; Zhao, J.; Van Duyne, R. P. *Nat. Mater.* **2008**, *7*, 442.
(27) Skadtchenko, B. O.; Aroca, R. *Spectrochim. Acta, Part A* **2001**, *57*, 1009.
(28) Kim, K.; Shin, D.; Lee, H. B.; Shin, K. S. *Chem. Commun.* **2011**, *47*, 2020.